

# Knockdown of lncRNA SSTR5-AS1 Regulates Ferroptosis and Immunosuppressive Factor Expression Through STAT3/SLC7A11 Signaling Pathway to Interfere with the Progression of Ovarian Cancer

Qiong Wei, Chun Wang, Yi Yang, Yuping Li, and Huan Huang

Department of Obstetrics and Gynecology, Wuhan Third Hospital (Tongren Hospital of Wuhan University), Wuhan, China

Received: 26 September 2025; Received in revised form: 6 January 2026; Accepted: 27 January 2026

## ABSTRACT

Long noncoding RNA SSTR5 antisense RNA 1 (lncRNA SSTR5-AS1) is increased in a variety of tumors, but its molecular mechanism in ovarian cancer (OC) remains unreported.

lncRNA SSTR5-AS1 and signal transducer and activator of transcription 3 (STAT3) expressions in SKOV3 and A2780 cells were interfered (n=3), and the cells were treated with ferroptosis inhibitor Ferrostatin-1. lncRNA SSTR5-AS1 and STAT3 expressions were discovered. The interaction between them was detected by immunoprecipitation assay. The cell malignant progression was evaluated through Transwell and scratch healing assays. Ferroptosis was measured through kits and fluorescent probes; the expression levels of immunosuppressive factors and STAT3/solute carrier family 7 member 11 (SLC7A11) signaling pathway were discovered through Western blot. A transplanted tumor model (n=6 mice per group) was established to evaluate ferroptosis, immunosuppressive factors, and tumor growth in tumor tissues.

lncRNA SSTR5-AS1 was up-regulated on OC cells. lncRNA SSTR5-AS1 and STAT3 bind to each other, and knockdown of lncRNA SSTR5-AS1 can reduce p-STAT3/STAT3 and SLC7A11 protein levels (one-way ANOVA). Knocking down lncRNA SSTR5-AS1 and STAT3 suppressed cell viability, migratory rate, and invasive cell number; increased reactive oxygen species (ROS) and Fe<sup>2+</sup> levels; and reduced immunosuppressive factors and ferroptosis proteins. Ferrostatin-1 significantly reversed the effect of knockdown of lncRNA SSTR5-AS1 on ferroptosis. In transplanted tumor tissues, downregulation of lncRNA SSTR5-AS1 can reduce tumor size and volume, show obvious iron deposition, and reduce the secretion of immunosuppressive factors.

Knockdown of lncRNA SSTR5-AS1 induces ferroptosis and reduces the secretion of immunosuppressive factors through the STAT3/SLC7A11 pathway, thereby antagonizing OC.

**Keywords:** Ferroptosis; Immunosuppression; Long non-coding RNA SSTR5-AS1; Ovarian neoplasms; SLC7A11 protein; STAT3 transcription factor

---

**Corresponding Authors:** Yuping Li: MD,  
Department of Obstetrics and Gynecology, Wuhan Third Hospital (Tongren Hospital of Wuhan University), Wuhan, China.  
Tel: (+86 150) 7239 1980, Fax: (+86 027) 6539 9961, Email: berry2005@163.com

---

Huan Huang, MB;  
Department of Obstetrics and Gynecology, Wuhan Third Hospital (Tongren Hospital of Wuhan University), Wuhan, China.  
Tel: (+86 153) 2720 8696, Fax: (+86 027) 6539 9961, Email: hhtj99-hh@hotmail.com

The first and second authors contributed equally to this study

## INTRODUCTION

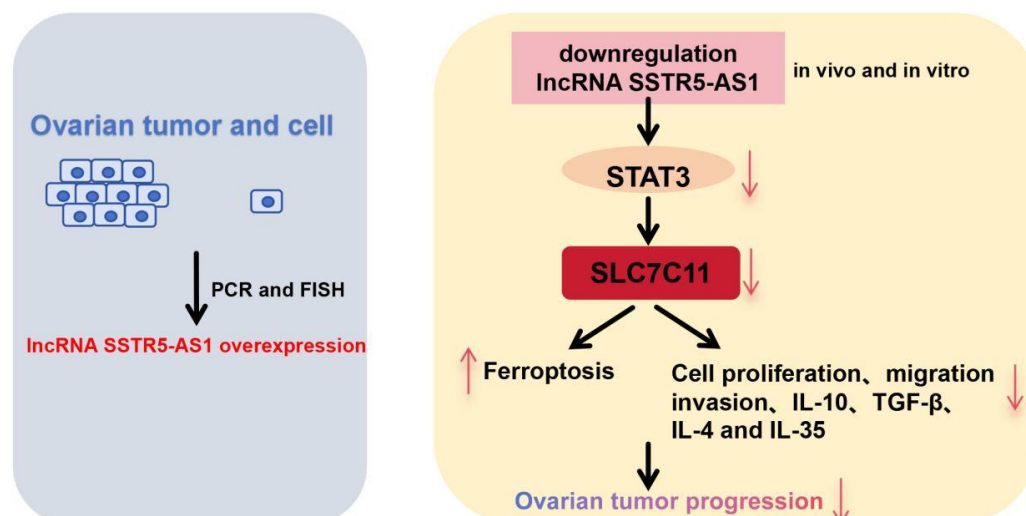
Ovarian cancer (OC) represents a major cause of death among malignant tumors in women,<sup>1,2</sup> and its diagnosis and treatment have always been the focus of gynecological tumor research. The number of new incidences in China is about 88 400 in 2022, and the number of deaths will be about 47 300. The incidence and mortality of OC have significantly increased.<sup>3</sup> Because OC frequently lacks visible symptomatology in its earlier stage<sup>4</sup> and lacks efficient early diagnosis tools, most OC patients are diagnosed at the later stages of the disease, which greatly reduces the effectiveness of treatment and patients' survival rates. OC treatment is a comprehensive treatment of surgery and adjuvant chemotherapy. The surgery is mainly to remove the tumor tissue by tumor reduction, and the chemotherapy is based on paclitaxel combined with carboplatin as the standard and preferred regimen. Although some progress has been made OC treatment recently, including chemotherapy, radiotherapy, and targeted therapies,<sup>5,6</sup> the therapeutic effect is still limited, and often accompanied by high recurrence rate and chemotherapy resistance.<sup>7</sup> Therefore, exploring new therapeutic mechanisms and therapeutic targets to improve treatment efficiency and reduce adverse reactions has become an urgent need in this field.

As a key mechanism for regulating cancer development and therapeutic response, the cell death pathway has recently received extensive attention. With deepening researches, ferroptosis has attracted the interest of researchers as a novel mode of cell death, especially in cancer treatment.<sup>8-10</sup> In the presence of iron ions, reactive oxygen species (ROS) in cells oxidize polyunsaturated fatty acids on the lipid membrane to produce lipid peroxides, causing membrane rupture and cell death.<sup>11</sup> Ferroptosis inhibits the proliferation of various tumor cells, including but not limited to OC.<sup>12</sup> Ferroptosis may influence OC progression by regulating the migration and invasion of tumors.<sup>13</sup> Iron ion transport and ferroptosis tolerance-related genes can enhance tumor cell multiplication and invasion through modulating the immune microenvironment and glutathione (GSH) redox status.<sup>14</sup> Induction of ferroptosis inhibits the progression of OC, so ferroptosis inducers are considered as potential anti-OC candidates.<sup>15</sup> In conclusion, induction of ferroptosis is a vital mechanism for OC treatment.

In tumorigenesis and progression, long non-coding RNA (lncRNA) can play a number of important roles in genomic stability, regulation of transcription, and epigenetics.<sup>16-18</sup> lncRNA is involved in the multiplication, movement, invasion, epithelial-mesenchymal transition (EMT), and other important processes of OC cells, its abnormal expressions are associated with negative prognosis of OC patients.<sup>19,20</sup> lncRNA SSTR5 antisense RNA 1 (SSTR5-AS1) is located in the 16p13.3 region and is an antisense transcript of SSTR5, a member of the somatostatin receptor superfamily. The SSTR gene family is a variety of tumor markers.<sup>21</sup> Studies have shown that lncRNA SSTR5-AS1 is involved in many tumors' occurrence (esophageal cancer, prostate cancer, gastric cancer).<sup>22-25</sup> lncRNA SSTR5-AS1 promotes the growth, EMT, and movement of cancer cells, and has a positive relationship with tumor progression, lymphatic node spread, and distant metastasis of tumors. Therefore, cancer patients with high lncRNA SSTR5-AS1 level tend to have worse prognosis. lncRNA SSTR5-AS1 may be similar for promoting cancer in different malignant tumors. However, the association of lncRNA SSTR5-AS1 with OC remains unreported.

lncRNA SSTR5-AS1 level of OC tissues and OC cells was detected. The influence of lncRNA SSTR5-AS1 in malignant biological behaviors of OC were investigated through a series of biological experiments. The possible mechanism of action was discussed from the perspective of ferroptosis, which provided a theoretical basis for OC early diagnosis and therapy.

## Knockdown of LncRN SSTR5-AS1 Interferes with Ovarian Cancer Progression



**Graphical Abstract.** Downregulation of lncRNA SSTR5-AS1 can induce ferroptosis of OC cells and inhibit immunosuppressive factors through STAT3/SLC7A11 pathway, thus inhibiting the progression of OC.

### MATERIALS AND METHODS

#### Organizational Samples

The fresh ovarian tissues of 60 patients with primary OC who were treated in Hospital were collected. All the selected patients were diagnosed as primary OC by pathological section and did not receive preoperative adjuvant therapy. Patients with other gynecological diseases and no ovarian involvement but ovarian resection were selected as controls, and 60 normal ovarian tissue samples were collected. This study was approved by the Ethics Committee, and all patients have signed informed consent.

#### Cell Culture and Infection

Human normal ovarian epithelial cells IOSE-80 and human OC cell lines (SKOV3, OVCAR-3, A2780, Caov-3, and HEY A8) were purchased from SUNNCELL (SNL-626, SNL-097, SNL-404, SNL-132, SNL-280, SNL-617, Wuhan, China). All purchased cells were quickly removed and placed in a 39.5 °C warm water bath for thawing and resuscitation, and cultured in RPMI-1640 medium (10% fetal bovine serum + 1% penicillin-streptomycin).

After SKOV3 and A2780 cells were inoculated in 24-well plates and cultured to logarithmic growth phase, they were randomly divided into overexpression of lncRNA SSTR5-AS1 (OE-SSTR5-AS1) group, knockdown of lncRNA SSTR5-AS1 (si-SSTR5-AS1)

group, overexpression of signal transducer and activator of transcription 3 (STAT3) (OE-STAT3) group, knockdown of STAT3 (si-STAT3) group, and corresponding negative control (OE-NC and si-NC) group. Each experimental group was transfected with liposome 3000: OE-SSTR5-AS1 group cells were transfected with OE-SSTR5-AS1, si-SSTR5-AS1 group cells were transfected with si-SSTR5-AS1, OE-STAT3 group cells were transfected with OE-STAT3, si-STAT3 group cells were transfected with si-STAT3, and negative control group cells were transfected with OE-NC and si-NC. The specific method is described in the Lipofectamine™ 3000 (L3000150, Invitrogen, USA) instruction. At 24 hours, reverse transcription quantitative real-time polymerase chain reaction (RT-qPCR) was used to quantify *lncRNA SSTR5-AS1* expression, while Western blot was used to assess STAT3 protein expression in each group.

Ferrosstatin-1 (Fer-1, Y240805, Beyotime, Shanghai, China), a ferroptosis inhibitor, was used to interfere with stably transfected SKOV3 and A2780 cells. Simultaneously, OC cells were intervened with 10 μM ferroptosis activator Erastin (Y240017, Beyotime) for 48 hours.

#### RT-qPCR

Total RNA was extracted from OC tissues, normal ovarian tissues, OC cells, and mouse tumor tissues using TransZol Up reagent (ET111-01-V2, TRANS, Beijing,

China). RNA purity and concentration were examined by ultramicro nucleic acid protein analyzer (Q5000, quawell, San Jose, CA, USA). RNA was reverse transcribed into cDNA by PrimeScript™ FAST RT reagent Kit with gDNA Eraser reverse transcription kit (RR092S, TAKARA, Tokyo, Japan). TB Green FAST qPCR (CN830S, TAKARA) was used for qPCR detection. The CT value was calculated; target gene expression calculation formula was  $= 2^{-\Delta\Delta CT}$ . *GAPDH* served as internal reference. *lncRNA SSTR5-AS1* F: 5'-ACTACAGGTGCCATCAGACC-3'; R: 5'-AGCCTGCCATCCTAACACTT-3'; *GAPDH* F: 5'-CTCTGCTCCTCCTGTTCGAC-3'; R: 5'-GCGCCCAATACGACCAAATC-3'.

### Fluorescent In Situ Hybridization (FISH)

*lncRNA SSTR5-AS1* expressions in SKOV3 and A2780 cells were examined using FISH probe and kit (C10910, RIBBIO, Guangzhou, China). The cell slides were pre-hybridized at 55 °C for 2 hours, and the samples were hybridized overnight at 37 °C using a specific FITC-labeled *lncRNA SSTR5-AS1* probe. After hybridization, the samples were nuclear stained with 4',6-diamidino-2-phenylindole (DAPI). Finally, the fluorescence signal was measured using confocal microscopy (LSM 910, Zeiss, Oberkochen, Germany).

### Cell Counting Kit-8 (CCK-8) Assay

After the intervention of SKOV3 and A2780 cells, 10 μL CCK-8 solution (G4103, Servicebio, Wuhan, China) was added. The optical density (OD) value at 450 nm wavelength was detected by microplate reader (Spectra Max-M5, Molecular Devices, San Jose, CA, USA). The detection was performed once every 24 hours, and the OD value of each detection was recorded. Cell multiplication curve was drawn to evaluate the cell proliferation ability.

In addition, OC cells were treated with 10 μL CCK-8 solution for 2 hours. The OD450 nm value of each group of cells was detected, and cell viability in each group was calculated.

### Transwell Experiment

According to the volume ratio of 1:8, Matrigel was diluted and then coated on the upper chamber membrane of the Transwell chamber. The stably transfected SKOV3 and A2780 cells in each group were digested with 0.25% trypsin for 5 minutes, centrifuged, removed the supernatant, washed twice with phosphate-buffered

saline (PBS), resuspended in serum-free medium, adjusted the cell concentration to  $1 \times 10^5$  cells/mL, and inoculated in the upper chamber (500 μL) of Matrigel. The lower chamber was added with culture medium (containing 10% fetal bovine serum). After 24 hours of culture, the chamber was taken out, fixed with 4% paraformaldehyde for 15 minutes, stained with 0.1% crystal violet for 20 minutes. The residual cells on the upper chamber surface were wiped off with sterile cotton swabs, transferred to a glass slide, sealed with neutral resin, and observed under a microscope (CKX31, Olympus, Tokyo, Japan). Five visual fields (upper, middle, lower, left, and right) were randomly selected for photographing and counting purple positive cells. The results were statistically analyzed.

Similarly, 500 μL cell suspension was inoculated into the Transwell chamber, and the upper chamber of the Transwell was not coated with Matrigel. Then, the cells were cultured according to the above steps, and the number of cells migrating to the lower chamber was counted under the microscope.

### Scratch Healing Experiment

The stably transfected SKOV3 and A2780 cells were seeded in 6-well plates and cultured for 24 hours. A straight line was drawn evenly in the hole with a 200 μL gun head, and photographed after adding serum-free medium. Then, the cells were cultured for 48 hours, and the images of the scratch area were captured by a microscope. The scratch areas were calculated by Image J software and the mobility was calculated.

### Calcein-AM/PI Staining

Calcein-AM/PI staining kit (G1707, Servicebio) was used to detect live/dead cells. After the SKOV3 and A2780 cells were cultured, they were centrifuged at 4500 r/min for 5 minutes. The supernatant was discarded, and the cells were washed twice with  $1 \times$  Assay Buffer. The cell precipitate was resuspended with 1 mL  $1 \times$  Assay Buffer, and 1 μL Calcein-AM was added in the dark. After mixing, the cells were incubated in the dark at 37 °C for 25 minutes, and then 5 μL PI was added in the dark. The cells were stained in the dark at room temperature for 5 minutes, and centrifuged to remove the dye solution and resuspended with PBS. Then live cells (cytoplasmic fluorescence is green) and dead cells (nuclear fluorescence is red) were observed by fluorescence microscopy (CX41-32RFL, Olympus).

## Knockdown of LncRN SSTR5-AS1 Interferes with Ovarian Cancer Progression

### Detection of ROS Levels

SKOV3 and A2780 cells were collected after the intervention, and then the fluorescent probe 2',7'-Dichlorodihydrofluorescein diacetate (DCFH-DA) was diluted with serum-free medium at 1:1000 according to the operation steps in the ROS detection kit (S0033S, Beyotime) instruction. Each group of cells was added 500  $\mu$ L of diluted probe, incubated for 20 minutes in the dark, and mixed upside down every 5 minutes. Finally, ROS levels in each group were measured using flow cytometry (NovoCyte D2040R, Eisen Biotechnology Co., Ltd., Jiangsu, China).

### Kit Detection

SKOV3 and A2780 cells were gathered, broken by ultrasound, and supernatant was centrifuged. Malondialdehyde (MDA) and GSH assay kits (G4300, G4305, Servicebio) were used to analyze the content of MDA and GSH according to the supplier's plan. The experimental operation was carried out following kit instructions. The OD values of each hole were detected by microplate reader, and the enzyme content of each group was calculated. They were normalized to the total protein content of each sample (measured using the bicinchoninic acid (BCA) protein assay kit), and the final level was expressed as  $\mu$ mol/mg protein or  $\mu$ mol/g protein.

### FerroOrange Fluorescent Probe

SKOV3 and A2780 cells were made into a single cell suspension and planted in 96-well plates of 6000 cells/well density. After 24 hours of culture in the cell incubator, the intervention was performed. Then the medium was removed. The FerroOrange working solution (G1727, Servicebio) with a concentration of 1  $\mu$ mol/L was added and cultured in the incubator for 30 minutes, and then observed and photographed by fluorescence microscope.

### RNA Immunoprecipitation (RIP)

Firstly, the antigen samples were prepared, and the cultured SKOV3 and A2780 cells were divided into Input group, IgG group, and STAT3 group. Protein A/G beads (80105G, Thermo Fisher, Waltham, MA, USA) were washed with RIP lysis buffer. The experimental group was incubated with 3  $\mu$ g signal transducer and activator of transcription 3 (STAT3) antibody (ab267373, Abcam, Cambridge, UK) at 4°C overnight, and the control group was incubated with IgG or no

antibody. The next day, the magnetic beads and supernatant were separated by a magnetic frame for 3 minutes, and the magnetic beads were washed with RIP buffer at 4°C for later use. RIP lysis buffer was added to the transfected SKOV3 and A2780 cells, and the supernatant was collected after centrifugation. An equal volume of supernatant was used as a protein IP input and RNA input sample. The remaining supernatant was incubated with STAT3 antibody-conjugated magnetic beads at 4°C for 3 hours to form RNA-protein complexes. RT-qPCR was used to detect the relative enrichment of *lncRNA SSTR5-AS1*; Western blot was used to detect the relative enrichment of STAT3 protein.

### Transplanted Tumor Mice

Twenty-four BALB/c female nude mice, weighing (16–20) g, 4 weeks of age, purchased from Sberfos Biotechnology Co., Ltd. (Beijing, China). This study has passed the ethical review of animal experiments (NO.2024-018). The experimental procedures and programs meet the ethical requirements of animal experiments.

OC mouse model was established by subcutaneous injection of SKOV3 cells ( $2 \times 10^5$  cells) transfected with each group in nude mice. According to the plasmid transfected by the cells, they were divided into sh-NC group, sh-SSTR5-AS1 group, OE-NC group, and OE-SSTR5-AS1 group, with 6 mice in each group. Randomization was performed using a computer-generated random number sequence according to the body weight of the mice to ensure unbiased grouping. After 5 weeks, the mice were sacrificed, and the tumor tissue was taken out and its quality was measured. The tumor volume ( $1/2 \times \text{length} \times \text{width}^2$ ,  $\text{mm}^3$ ) was calculated weekly. During the experimental period, the investigator responsible for measuring tumor dimensions (length and width) and body weight was blinded to group assignment to minimize observer bias. Histopathological evaluation of tumor samples was also conducted in a blinded manner by an independent researcher.

### Immunohistochemistry

The tumor tissues were collected, fixed with 4% paraformaldehyde, embedded in paraffin, and sliced at 5  $\mu$ m thickness. Paraffin sections were dewaxed and hydrated, incubated with 3%  $\text{H}_2\text{O}_2$  for 10 minutes to eliminate the activity of endogenous peroxidase, blocked with 5% bovine serum albumin (BSA) for 10 minutes, dropped with primary antibody Ki-67

(ab279653, 1:50, Abcam), incubated at 37°C for 1 hour, dropped with an appropriate amount of secondary antibody working solution, incubated at 37°C for 10 minutes, 3,3'-Diaminobenzidine (DAB) solution coloration, hematoxylin counterstaining, neutral gum sealing. Nuclear and cytoplasmic staining was brownish yellow or brown as positive, and non-overlapping fields were randomly selected. The stained sections were assessed microscopically and photographed.

### ROS Levels in Tumor Tissues

The production of ROS was evaluated by DCFH-DA staining (CA1410, Solarbio, Beijing, China). The fresh frozen sections of the tumor were stained with DCFH-DA probe working solution for 30 minutes in the dark. The sections were washed with PBS for 3 times. Finally, the fluorescence intensity was observed under a fluorescence microscope and photographed, it was analyzed by Image J software.

### Prussian Blue Staining

After dehydration and dewaxing of tumor paraffin sections, Prussian blue staining solution was stained for 30 minutes, and nuclear fast red staining solution was stained for 5 minutes. After soaking in gradient ethanol and xylene for 10 seconds, the neutral resin seal was added dropwise. After the resin solidified, it was observed and photographed.

### Enzyme-Linked Immunosorbent Assay (ELISA) Experiment

Tumor tissue was homogenized with normal saline, and the supernatant was collected after centrifugation (4 °C, 10 000 r/min, 10 minutes). The contents of interleukin (IL)-10, transforming growth factor- $\beta$  (TGF- $\beta$ ), IL-4, and IL-35 in tumor tissues were examined through ELISA kit (H009-1-2, H034-1-1, H005-1-2, H375-1, Jiancheng Bioengineering Institute, Nanjing, China). The specific steps were carried out according to the instructions: the standard and the sample to be tested were added to the kit, and incubated for 60 minutes; the plate was added with enzyme-labeled secondary antibody, and incubated for 60 minutes. The color development solution was added, and termination solution was added after 15 minutes. The OD450 nm value was measured. The color depth was proportional to the content of the analyte in the sample. IL-10, TGF- $\beta$ , IL-4, and IL-35 contents were calculated by plotting the standard curve.

### Western Blot

Tumor tissues and SKOV3 and A2780 cells were collected from each group. Radioimmunoprecipitation assay (RIPA) lysate (containing 1% protease inhibitor and phosphatase inhibitor) was added to extract total protein, and BCA protein concentration detection kit (P0009, Beyotime) was used for protein quantitative analysis. After boiling denaturation, the protein sample was separated by 10% sodium dodecyl sulfate-polyacrylamide gel electrophoresis (SDS-PAGE) pre-gel electrophoresis, and the protein was transferred to polyvinylidene difluoride (PVDF) membrane. The membrane was blocked overnight at room temperature with TBST containing 5% skim milk, and incubated overnight at 4 °C with diluted primary antibodies. IgG-HRP-labeled secondary antibodies (ab97080, Abcam) were added and incubated for 1 hour. The PVDF membrane was placed on an imaging analysis system (ChemiDoc XRS+, BIO-RAD, Hercules, CA, USA), and the target strip was developed by enhanced chemiluminescence (ECL) chemiluminescence. ImageJ software was used to quantify the gray scale of each protein and calculate its ratio to the internal reference GAPDH. The relative expressions of proteins were obtained by statistical analysis.

Antibodies used: Matrix metalloproteinase (MMP)-2 (ab181286, abcam), solute carrier family 7 member 11 (SLC7A11, ab307601, abcam), MMP-9 (ab58803, abcam), IL-10 (ab133575, abcam), TGF- $\beta$  (ab315254, abcam), IL-4 (ab62351, abcam), IL-35 (ICA008Mu01, LMAI Bio, Shanghai, China), nuclear factor erythroid 2-related factor 2 (Nrf2, AF7623, Beyotime), ferritin heavy chain 1 (FTH1, ab65080, abcam), glutathione peroxidase 4 (GPX4, ab219592, abcam), STAT3 (ab109085, abcam), p-STAT3 (ab76315, abcam), and GAPDH (ab181603, 1:10 000, abcam), dilution rate 1:1000.

### Statistical Analysis

Statistical analysis was conducted using SPSS version 27.0. For all datasets, normality was assessed using the Shapiro-Wilk test, and homogeneity of variances was verified using Levene's test. If data met the assumptions of normality and homogeneity of variance, one-way ANOVA was utilized, followed by Tukey's post hoc test for group comparisons. If data were non-parametric, the Kruskal-Wallis test was used for overall comparisons across groups, followed by Dunn's post hoc test for pairwise comparisons. The

## Knockdown of LncRN SSTR5-AS1 Interferes with Ovarian Cancer Progression

False Discovery Rate (FDR) was used to control the false positive rate when multiple independent indicators were analyzed simultaneously. Data for each group were presented as mean  $\pm$  standard deviation, with  $p < 0.05$  deemed statistically significant. Each mean value was derived from a minimum of three independent experiments.

### RESULTS

#### LncRNA SSTR5-AS1 Was Up-Regulated on OC Tissues and Cells

To determine the action of lncRNA SSTR5-AS1 on OC, 60 tumor tissues of OC patients and 60 normal

ovarian tissues were gathered in this study. RT-qPCR results found that *lncRNA SSTR5-AS1* level on OC tissues was notably high, increasing by 2.16 times (Figure 1A). *lncRNA SSTR5-AS1* was expressed in IOSE-80 and five OC cell lines (SKOV3, OVCAR-3, A2780, Caov-3, and HEY A8), and *lncRNA SSTR5-AS1* level on OC cell lines was markedly high (Figure 1B). Because *lncRNA SSTR5-AS1* has the highest expression level in SKOV3 and A2780 cells, these two cells chosen for following experiments. FISH results showed that the signal of lncRNA SSTR5-AS1 probe labeling could be detected in the cytoplasm (Figure 1C), indicating that lncRNA SSTR5-AS1 existed in the cytoplasm of OC.

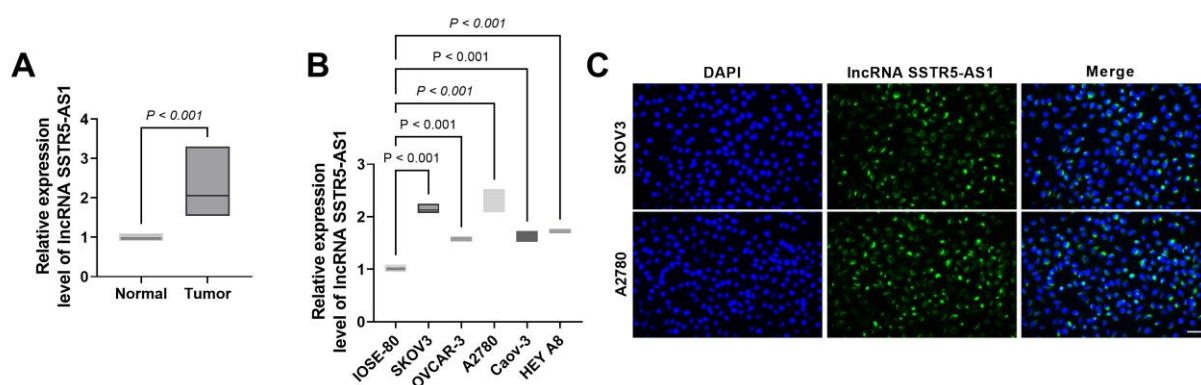


**Figure 1.** LncRNA SSTR5-AS1 was up-regulated on OC tissues and cells. **A**, Sixty fresh OC tissue samples and normal ovarian tissues were collected, and *lncRNA SSTR5-AS1* expressions were measured through RT-qPCR. *lncRNA SSTR5-AS1* level was up-regulated on OC tissues. **B**, RT-qPCR measured *lncRNA SSTR5-AS1* expressions of IOSE-80 and OC cells (SKOV3, OVCAR-3, A2780, Caov-3, and HEY A8). *lncRNA SSTR5-AS1* level was increased in OC cells. **C**, FISH assessed *lncRNA SSTR5-AS1* expressions on SKOV3 and A2780 cells ( $\times 20$ , 100  $\mu\text{m}$ ).  $n=3$ ,  $**p < 0.01$ ,  $***p < 0.001$  vs Normal/IOSE-80 group.

#### Knocking Down LncRNA SSTR5-AS1 Suppressed OC Cell Multiplication, Movement, Invasion, and Immunosuppressive Factor Expression

Since lncRNA SSTR5-AS1 is increased on OC, we speculate that knockdown of lncRNA SSTR5-AS1 may help to inhibit OC progression. To this end, this study interfered with lncRNA SSTR5-AS1 expressions on SKOV3 and A2780 cells, and transfected OE-SSTR5-AS1, si-SSTR5-AS1, and the corresponding negative control into OC cells, respectively. OE-SSTR5-AS1 significantly increased *lncRNA SSTR5-AS1* expression (SKOV3 cells: increased by 2.91 times; A2780 cells: increased by 2.64 times), and si-SSTR5-AS1 significantly decreased *lncRNA SSTR5-AS1* expression (SKOV3 cells: reduced by 55%; A2780 cells: reduced

by 49%) (Figure 2A), indicating successful overexpression or knockdown of lncRNA SSTR5-AS1. After overexpression of lncRNA SSTR5-AS1, the cell viability increased significantly, migration and invasion cell numbers increased significantly, the cell migration rate in scratch healing experiment also increased significantly (Figure 2B–I), indicating that lncRNA SSTR5-AS1 overexpressed could enhance OC cell growth, movement, and invasion. Knockdown of lncRNA SSTR5-AS1 had the opposite effect. After that, Calcein-AM/PI staining distinguished live cells from dead cells, and the effects of lncRNA SSTR5-AS1 in cell viability was evaluated. The green fluorescence of living cells is due to the conversion of calcein acetyloxy methyl ester to calcein, and PI only stains dead cells to

produce red fluorescence. The cells under the fluorescence microscope are shown in Figure 2J–K. Many normal cells-stained green were observed in the OE-SSTR5-AS1 group. The living cells in the si-SSTR5-AS1 group were significantly reduced, and the dead cells labeled with red fluorescence were significantly increased. Finally, MMPs are associated with cancer cell invasion and metastasis. IL-10, TGF- $\beta$ , IL-4, and IL-35 are important for limiting anti-tumor immunity and tumor growth and progression. After overexpression of lncRNA SSTR5-AS1, MMP-2 (SKOV3 cells: increased by 2.16 times; A2780 cells: increased by 1.76 times) and MMP-9 (SKOV3 cells: increased by 2.35 times; A2780 cells: increased by 2.14 times) expressions were markedly raised, and IL-10 (SKOV3 cells: increased by 2.33 times; A2780 cells: increased by 2.03 times), TGF- $\beta$  (SKOV3 cells: increased by 2.11 times; A2780 cells: increased by 2.25 times), IL-4 (SKOV3 cells: increased by 3.00 times; A2780 cells: increased by 2.23 times), and IL-35 (SKOV3 cells: increased by 2.09 times; A2780 cells: increased by 2.02 times) levels were also markedly raised (Figure 2L–R), indicating that overexpression of lncRNA SSTR5-AS1 could not only enhance cell migration and invasion, but also promote the expression of immunosuppressive factors. Conversely, knockdown of lncRNA SSTR5-AS1 inhibited immunosuppressive factors in OC cells. In conclusion, knocking down lncRNA SSTR5-AS1 blocked the expression of immunosuppressive cytokines, activated anti-tumor immunity, and inhibited OC cell malignant progression.

#### **Knockdown of lncRNA SSTR5-AS1 Caused Ferroptosis on OC Cells**

To clarify the role of ferroptosis in the antagonistic effects of knockdown of lncRNA SSTR5-AS1 on OC, this study used ferroptosis inhibitor Fer-1 and activator Erastin to intervene in OC cells. Compared with the si-SSTR5-AS1 group, the cell viability was significantly increased after Fer-1 intervention (Figure 3A), suggesting that Fer-1 weakened the effect of si-SSTR5-AS1, indicating that knockdown of lncRNA SSTR5-AS1 activated the ferroptosis pathway to reduce OC cell viability. After lncRNA SSTR5-AS1 knockdown and Erastin intervention, ROS and MDA levels increased significantly, and the activity of GSH decreased significantly. After Fer-1 intervention, ROS (SKOV3 cells: reduced by 51%; A2780 cells: reduced by 46%) and MDA (SKOV3 cells: reduced by 53%; A2780 cells:

reduced by 48%) levels were notably lessened, and GSH activity was notably elevated (SKOV3 cells: increased by 68%; A2780 cells: increased by 56%) (Figure 3B–E). The fluorescence signal labeled by FerroOrange fluorescent probe also increased significantly after lncRNA SSTR5-AS1 knockdown and Erastin intervention, and decreased significantly after Fer-1 intervention (Figure 3F–G), indicating that knocking down lncRNA SSTR5-AS1 markedly increased Fe<sup>2+</sup> content in cells. Nrf2, SLC7A11, FTH1, and GPX4 are key indicators of ferroptosis.<sup>26,27</sup> Nrf2, SLC7A11, FTH1, and GPX4 levels were significantly decreased after lncRNA SSTR5-AS1 knockdown (Nrf2: reduced by 48% and 52%; SLC7A11: reduced by 56% and 48%; FTH1: reduced by 52% and 42%; GPX4: reduced by 56% and 47%) and Erastin intervention (Nrf2: reduced by 59% and 59%; SLC7A11: reduced by 54% and 54%; FTH1: reduced by 57% and 53%; GPX4: reduced by 62% and 63%), and significantly increased after Fer-1 intervention (Nrf2: increased by 1.66 and 1.76 times; SLC7A11: increased by 2.05 and 1.72 times; FTH1: increased by 1.83 and 1.48 times; GPX4: increased by 1.97 and 1.66 times) (Figure 3H–L). Knockdown of lncRNA SSTR5-AS1 reduced the antioxidant capacity of cells, increased lipid peroxidation and Fe<sup>2+</sup> aggregation, and promoted ferroptosis in OC cells.

## Knockdown of LncRN SSTR5-AS1 Interferes with Ovarian Cancer Progression

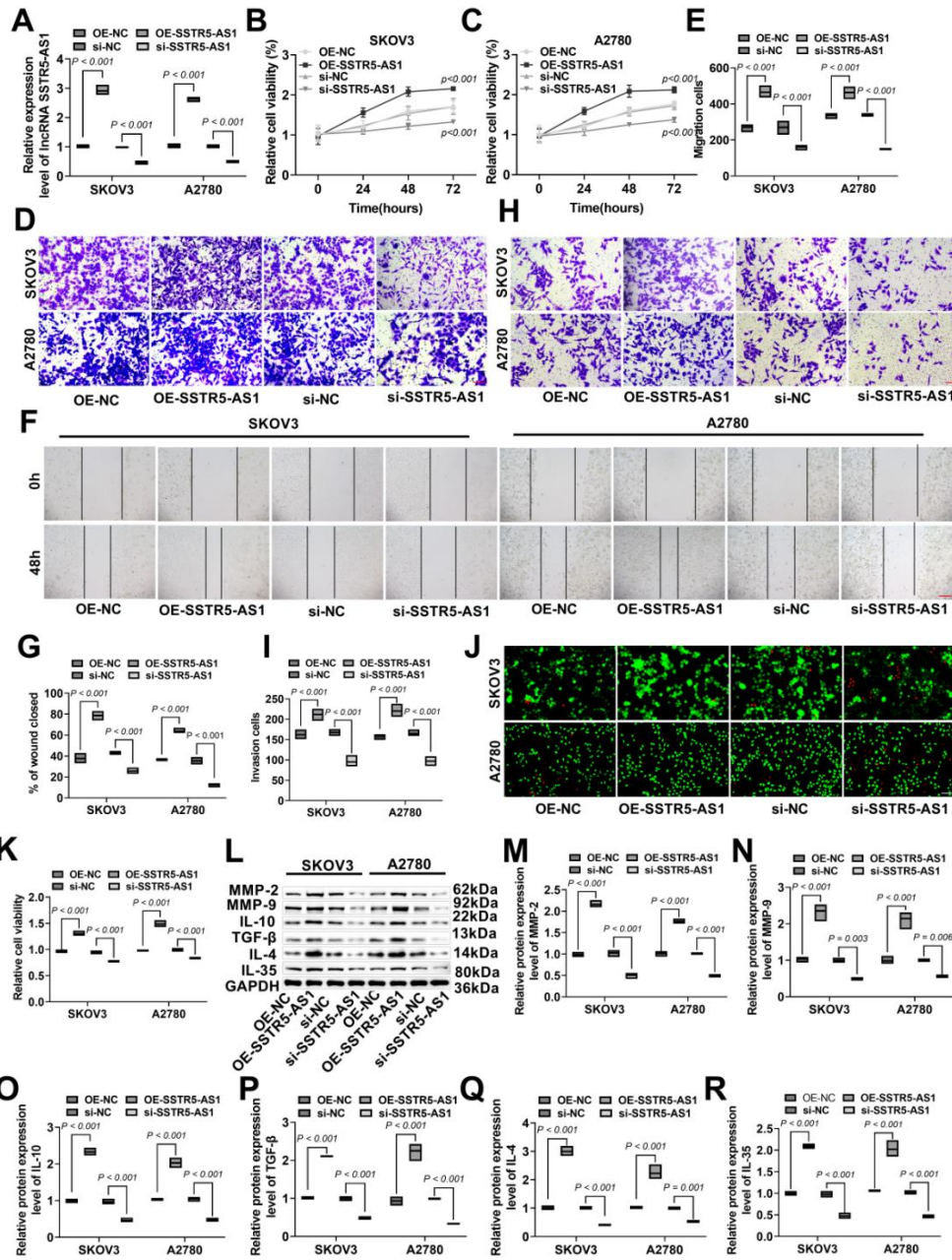


**Figure 2.** Knockdown of lncRNA SSTR5-AS1 inhibited OC cell multiplication, movement, invasion, and immunosuppressive factor expression. A, OE-SSTR5-AS1, si-SSTR5-AS1, OE-NC, and si-NC were transfected into SKOV3 and A2780 cells. The transfection efficiencies were examined using RT-qPCR. B–C, the cell viability of SKOV3 and A2780 cells was detected by CCK-8 assay. si-SSTR5-AS1 significantly inhibited cell viability. D–E, Transwell experiment detected cell migration. si-SSTR5-AS1 notably reduced the migrated cell number ( $\times 20$ , 100  $\mu\text{m}$ ). F–G, the cell migratory rate was examined through scratch healing experiment, which was significantly reduced after lncRNA SSTR5-AS1 knockdown ( $\times 10$ , 200  $\mu\text{m}$ ). H–I, Transwell experiment detected cell invasion. si-SSTR5-AS1 notably reduced the invasive cell number ( $\times 20$ , 100  $\mu\text{m}$ ). J–K, Calcein-AM/PI staining evaluated SKOV3 and A2780 cell survival. After lncRNA SSTR5-AS1 knockdown, the number of live cell models decreased and the number of dead cells increased significantly ( $\times 20$ , 100  $\mu\text{m}$ ). L–R, Western blot detected invasion, migration, and immunosuppressive proteins. MMP-2, MMP-9, IL-10, TGF- $\beta$ , IL-4, and IL-35 levels decreased after lncRNA SSTR5-AS1 knockdown.  $n=3$ ,  $***p < 0.001$  vs OE-NC group;  $\#p < 0.05$ ,  $\#\#p < 0.01$ ,  $\#\#\#p < 0.001$  vs si-NC group.

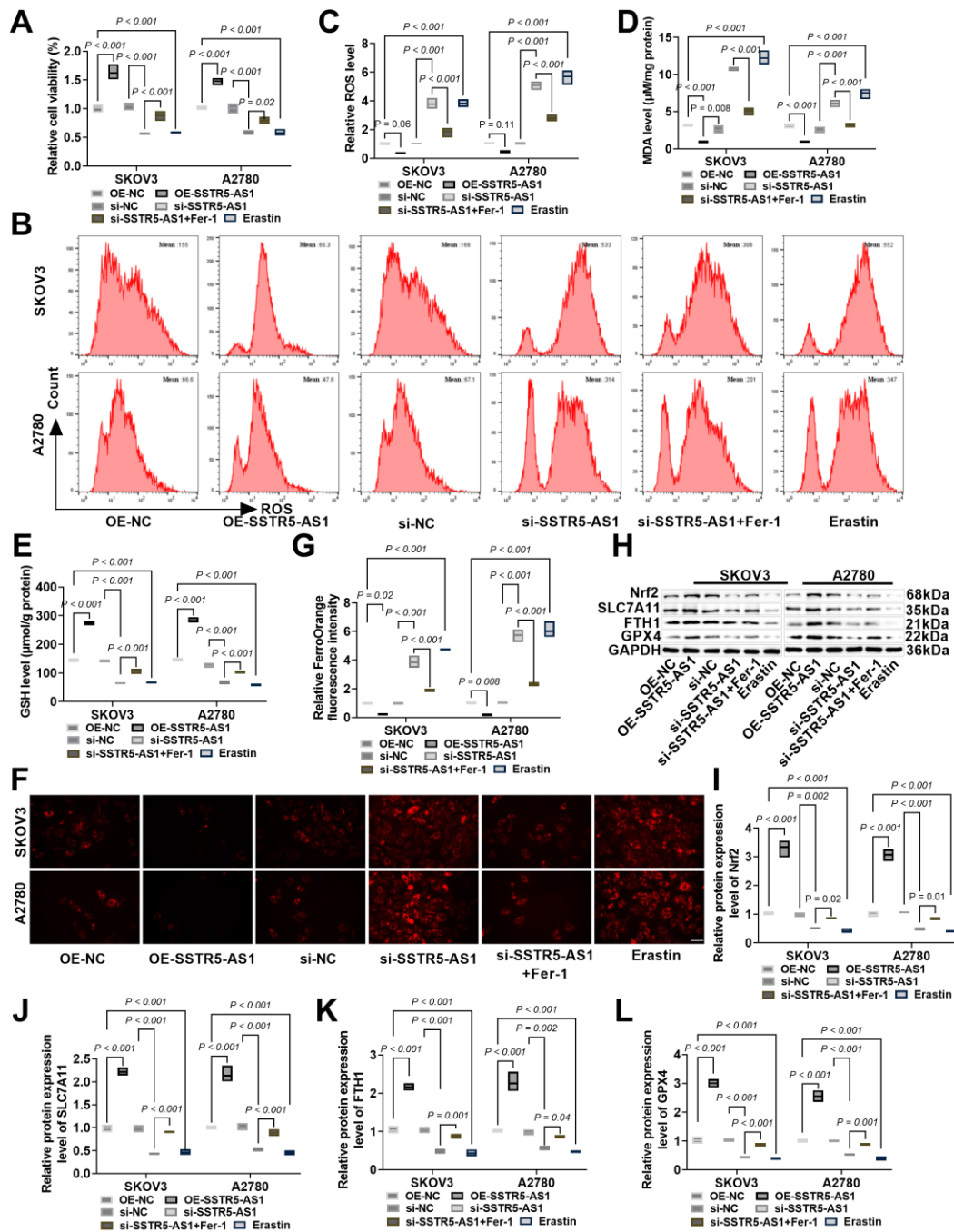


**Figure 3.** Knockdown of lncRNA SSTR5-AS1 caused ferroptosis on OC cells. **A**, SKOV3 and A2780 cells were intervened using 1 µM ferroptosis inhibitor Fer-1 and 10 µM ferroptosis activator Erastin. CCK-8 experiment detected cell proliferation. It was significantly increased after Fer-1 intervention. **B–C**, Flow cytometry evaluated ROS level. si-SSTR5-AS1 significantly increased ROS levels. **D–E**, MDA level and GSH activity in cells were detected by kit. si-SSTR5-AS1 significantly increased MDA level and inhibited GSH activity. **F–G**, FerroOrange fluorescent probe detected the content of Fe<sup>2+</sup> in cells, which was significantly increased after lncRNA SSTR5-AS1 knockdown (×40, 50 µm). **H–L**, Western blot detected ferroptosis-related protein expressions. Nrf2, SLC7A11, FTH1, and GPX4 protein levels were significantly declined after lncRNA SSTR5-AS1 knockdown. n=3, \*\*\*p<0.001 vs OE-NC group; ##p<0.01, ###p<0.001 vs si-NC group; &p<0.01, &&p<0.001 vs si-SSTR5-AS1 group.

### **Knockdown of lncRNA SSTR5-AS1 Inhibited STAT3/SLC7A11 Pathway Activation on OC Cells**

JAK2/STAT3 pathway is activated in hepatocellular carcinoma. Activation of STAT3 enhances SLC7A11 expression in cells and inhibits ferroptosis.<sup>28</sup> Therefore, we investigated whether lncRNA SSTR5-AS1 is involved in ferroptosis of OC cells mediated by STAT3/SLC7A11 signaling pathway. In the RIP experiment, STAT3 protein was measured in both Input group and RIP-STAT3 group, but not in the corresponding IgG group. lncRNA SSTR5-AS1 was detected in RIP products. Compared with RIP-IgG group, the content of RIP-STAT3 group was significantly higher (Figure 4A–B), indicating that there was an interaction between lncRNA SSTR5-AS1 and STAT3. p-STAT3/STAT3 and SLC7A11 protein expressions increased significantly after overexpression of lncRNA SSTR5-AS1 (p-STAT3/STAT3: increased by 1.62 and 1.67 times; SLC7A11: increased by 1.49 and 1.52 times), and decreased significantly after knockdown of lncRNA SSTR5-AS1 (p-STAT3/STAT3: decreased by 52% and 50%; SLC7A11: decreased by 40% and 41%) (Figure 4C–E), indicating that knockdown of lncRNA SSTR5-AS1 might help to inhibit STAT3/SLC7A11 signaling pathway. After that, this study interfered with STAT3 expression in OC cells. OE-STAT3 significantly raised p-STAT3/STAT3 and SLC7A11 proteins, while si-STAT3 significantly lessened p-STAT3/STAT3 and SLC7A11 proteins (Figure 4F–H). Compared with lncRNA SSTR5-AS1 knockdown, p-STAT3/STAT3 and SLC7A11 proteins were markedly raised when STAT3 overexpression (p-STAT3/STAT3: increased by 1.37 and 1.46 times; SLC7A11: increased by 1.58 and 1.67 times) and significantly lessened when STAT3 knockdown (p-STAT3/STAT3: decreased by 52% and 57%; SLC7A11: decreased by 54% and 53%) (Figure 4I–K). In summary, knockdown of lncRNA SSTR5-AS1 inhibited STAT3/SLC7A11 pathway in OC cells.

### **Knockdown of lncRNA SSTR5-AS1 Induced Ferroptosis in OC Cells Through STAT3/SLC7A11 Signaling Pathway**

In addition, compared with lncRNA SSTR5-AS1 knockdown, after STAT3 overexpression, ROS and MDA levels were significantly reduced, GSH activity was significantly increased (Figure 5A–D), and FerroOrange fluorescent probe-labeled Fe<sup>2+</sup> content was

also significantly reduced (Figure 5E–F), indicating that STAT3 overexpression could weaken the effect of lncRNA SSTR5-AS1 knockdown on ferroptosis. After STAT3 knockdown, ROS, MDA, and Fe<sup>2+</sup> levels were markedly raised, and GSH activity was significantly lessened (Figure 5A–F), indicating that inhibition of STAT3/SLC7A11 signaling pathway induced ferroptosis in OC cells. Western blot findings further confirmed this conclusion. Nrf2, FTH1, and GPX4 expressions increased significantly after STAT3 overexpression (Nrf2: increased by 3.15 and 2.04 times; FTH1: increased by 1.88 and 1.74 times; GPX4: increased by 2.02 and 2.04 times) and decreased significantly after STAT3 knockdown (Nrf2: reduced by 44% and 52%; FTH1: reduced by 68% and 56%; GPX4: reduced by 61% and 55%) (Figure 5G–J). Knockdown of lncRNA SSTR5-AS1 could inhibit STAT3/SLC7A11 signaling pathway and induce ferroptosis.

### **Knocking Down lncRNA SSTR5-AS1 Suppressed OC Cell Multiplication, Movement, Invasion, and Immunosuppressive Factor Expression Through STAT3/SLC7A11 Signaling Pathway**

This study also found that compared with lncRNA SSTR5-AS1 knockdown, OE-STAT3 markedly raised SKOV3 and A2780 cell viability (Figure 6A), migration and invasion cell numbers, and the migration rate in scratch healing assay (Figure 6B–G); however, si-STAT3 significantly inhibited cell malignant progression. MMP-2, MMP-9, IL-10, TGF- $\beta$ , IL-4, and IL-35 protein levels were notably raised after STAT3 overexpression (MMP-2: increased by 1.91 and 1.77 times; MMP-9: increased by 1.99 and 2.21 times; IL-10: increased by 2.29 and 1.92 times; TGF- $\beta$ : increased by 1.26 and 1.45 times; IL-4: increased by 1.91 and 2.10 times; IL-35: increased by 1.94 and 1.80 times) and significantly decreased after STAT3 knockdown (MMP-2: reduced by 52% and 44%; MMP-9: reduced by 49% and 51%; IL-10: reduced by 56% and 54%; TGF- $\beta$ : reduced by 51% and 46%; IL-4: reduced by 64% and 65%; IL-35: reduced by 64% and 66%) (Figure 6H–N). In conclusion, knockdown of lncRNA SSTR5-AS1 attenuated OC cell malignant progression via inhibiting STAT3/SLC7A11 signaling and blocking the expression of immunosuppressive cytokines.

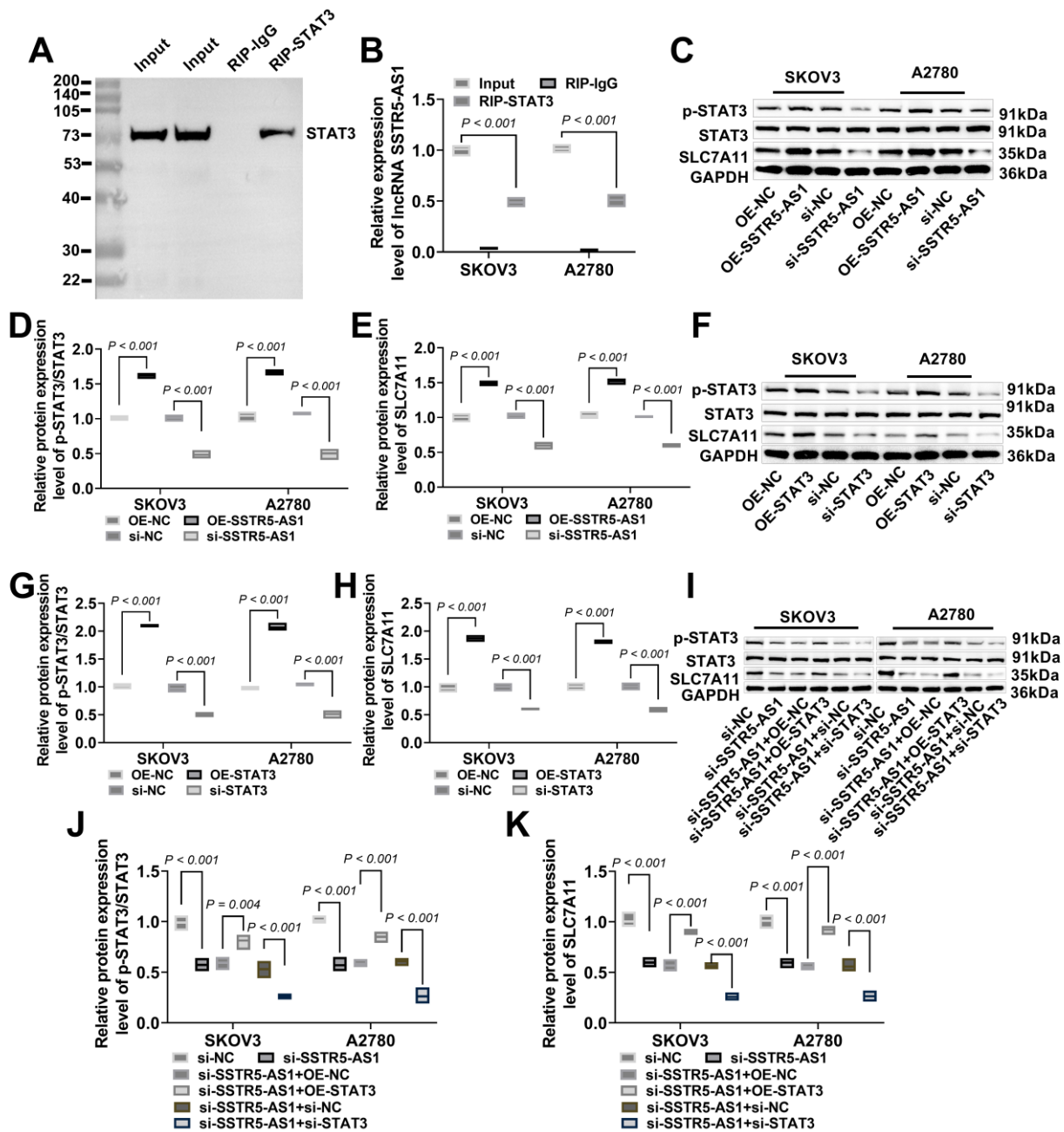


**Figure 4.** Knockdown of lncRNA SSTR5-AS1 inhibited STAT3/SLC7A11 pathway in OC cells. A–B, RIP assay verified the interaction between lncRNA SSTR5-AS1 and STAT3. C–E, Western blot detected STAT3/SLC7A11 pathway proteins. p-STAT3/STAT3 and SLC7A11 levels were notably decreased when lncRNA SSTR5-AS1 knockdown. F–H, OE-STAT3, si-STAT3, and corresponding negative control plasmids were transfected into SKOV3 and A2780 cells, and STAT3/SLC7A11 pathway protein expressions were measured through Western blot. I–K, lncRNA SSTR5-AS1 and STAT3 expressions in OC cells was simultaneously interfered, and then STAT3/SLC7A11 pathway proteins were measured through Western blot. n=3, \*\*\* $p < 0.001$  vs OE-NC/si-NC group; ## $p < 0.01$ , ### $p < 0.001$  vs si-NC/si-SSTR5-AS1+OE-NC group; &&& $p < 0.001$  vs si-SSTR5-AS1+si-NC group.

## Knockdown of LncRN SSTR5-AS1 Interferes with Ovarian Cancer Progression

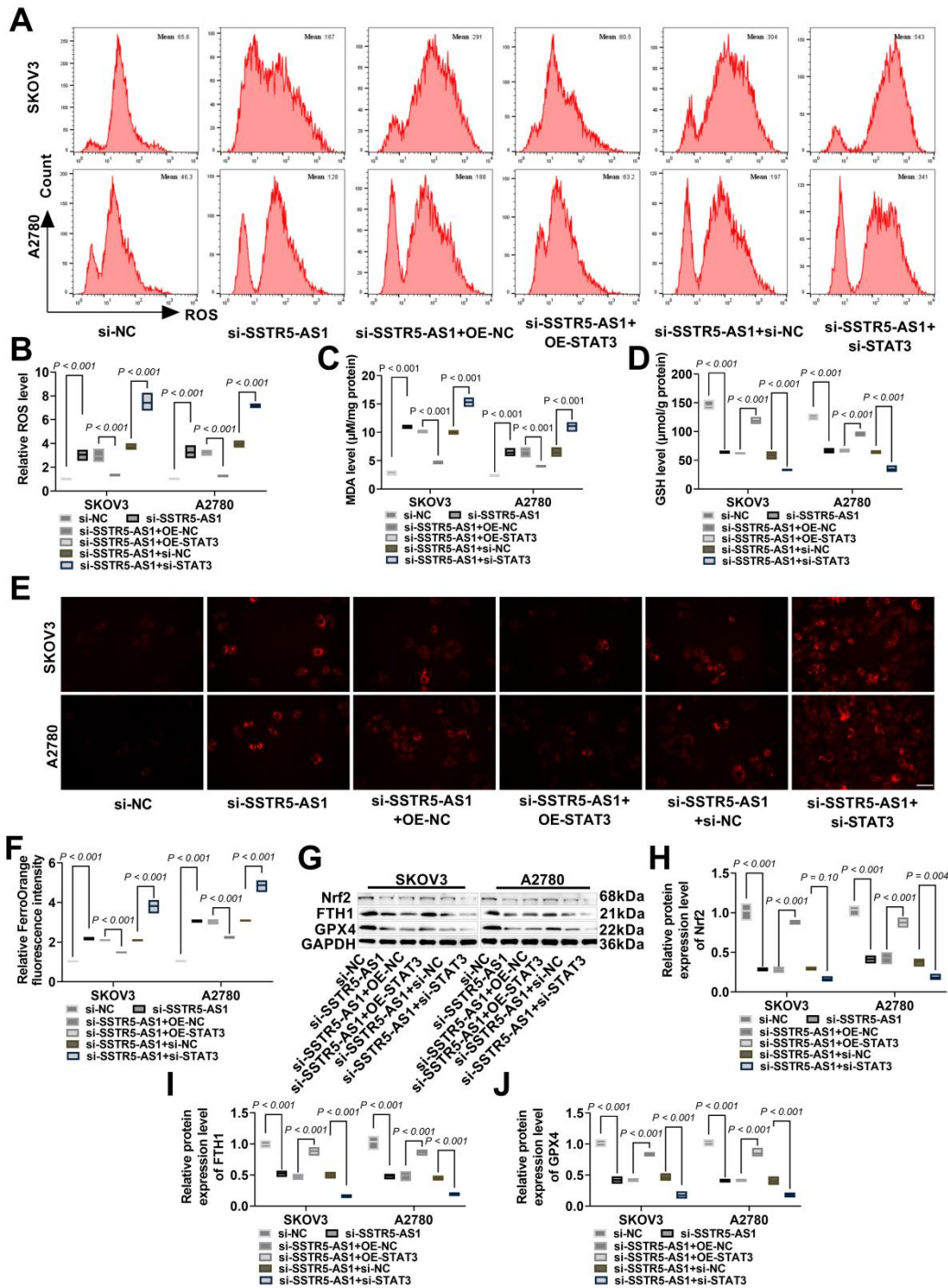


**Figure 5.** Knockdown of lncRNA SSTR5-AS1 induced ferroptosis in OC cells through STAT3/SLC7A11 signaling pathway. A–B, Flow cytometry evaluated ROS level. si-STAT3 significantly increased ROS levels. C–D, MDA level and GSH activity in cells were detected by kit. si-STAT3 significantly increased MDA level and inhibited GSH activity. E–F, FerroOrange fluorescent probe detected the content of Fe<sup>2+</sup>, which was significantly increased after STAT3 knockdown (×40, 50 μm). G–J, Western blot detected ferroptosis-related protein expressions. Nrf2, FTH1, and GPX4 protein expressions was significantly lessened after STAT3 knockdown. n=3, \*\*\*p<0.001 vs si-NC group; #p<0.05, ##p<0.01, ###p<0.001 vs si-SSTR5-AS1+OE-NC group; &&p<0.01, &&&p<0.001 vs si-SSTR5-AS1+si-NC group.

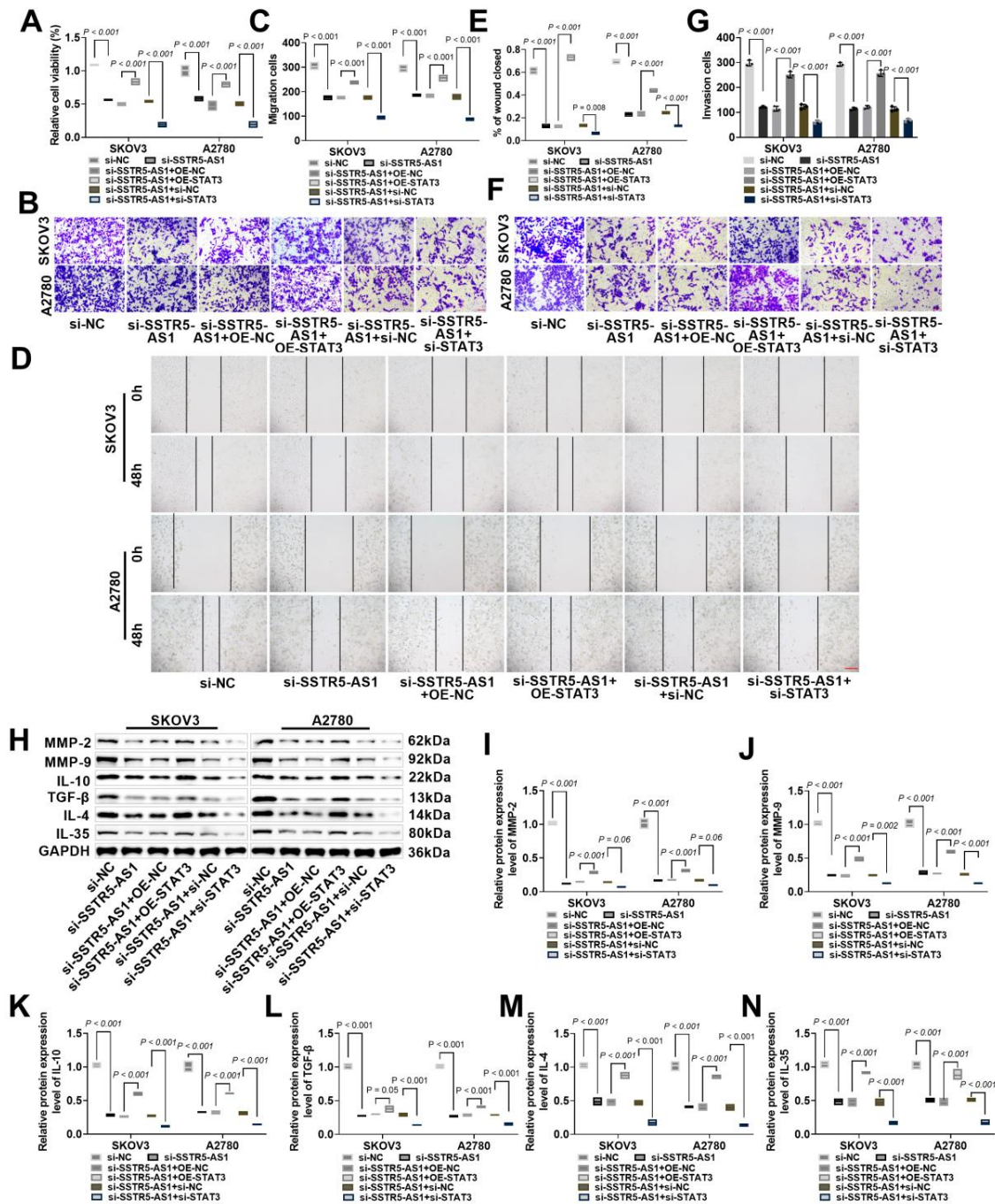
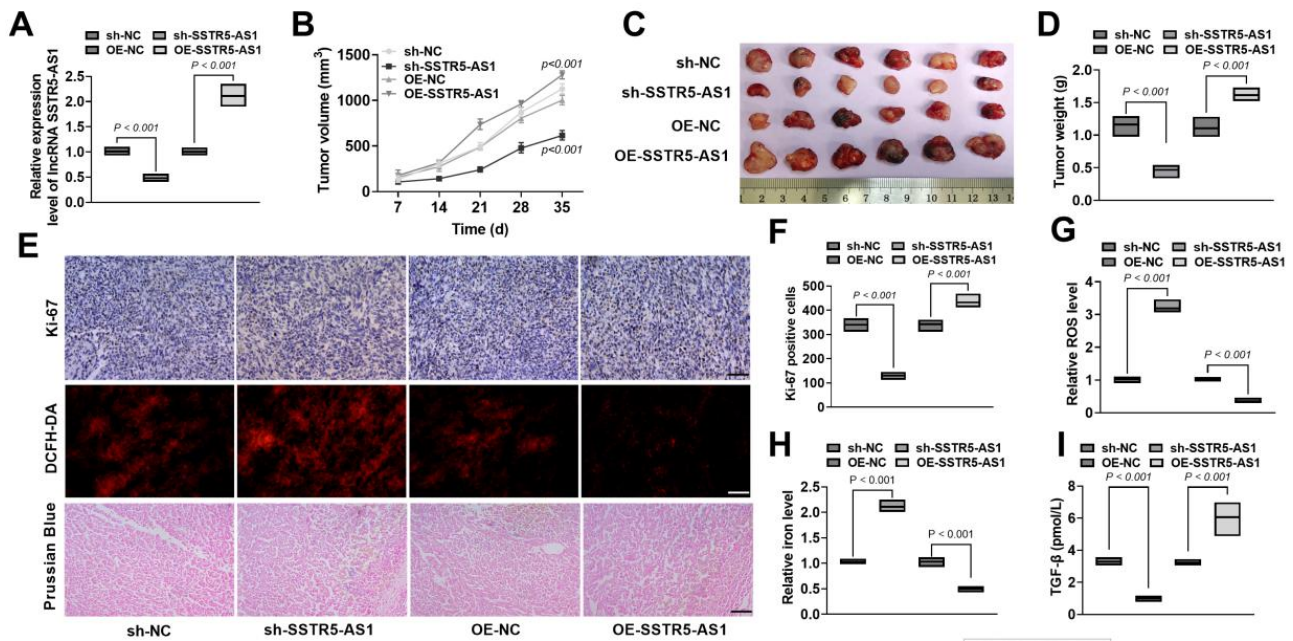


**Figure 6.** Knocking down lncRNA SSTR5-AS1 suppressed OC cell multiplication, movement, invasion, and immunosuppressive factor expression through STAT3/SLC7A11 signaling pathway. **A**, the cell viability of SKOV3 and A2780 cells was detected by CCK-8 experiment. si-STAT3 significantly inhibited cell viability. **B–C**, Transwell experiment detected cell migration. si-STAT3 obviously reduced the migrating cell number ( $\times 20, 100 \mu\text{m}$ ). **D–E**, the cell migratory rate was examined through scratch healing experiment, which was significantly reduced after STAT3 knockdown ( $\times 20, 100 \mu\text{m}$ ). **F–G**, Transwell experiment detected cell invasion. si-STAT3 obviously reduced the invasive cell number ( $\times 20, 100 \mu\text{m}$ ). **H–N**, Western blot detected invasion, migration, and immunosuppressive proteins. MMP-2, MMP-9, IL-10, TGF- $\beta$ , IL-4, and IL-35 levels decreased after STAT3 knockdown.  $n=3$ ,  $**p<0.01$ ,  $***p<0.001$  vs si-NC group;  $\#p<0.05$ ,  $\#\#p<0.01$ ,  $\#\#\#p<0.001$  vs si-SSTR5-AS1+OE-NC group;  $\&p<0.05$ ,  $\&\&p<0.01$ ,  $\&\&\&p<0.001$  vs si-SSTR5-AS1+si-NC group.

**Downregulation of lncRNA SSTR5-AS1 Inhibited the Activation of STAT3/SLC7A11 Signaling Axis, Induced Ferroptosis, Reduced the Secretion of Immunosuppressive Factors, and Suppressed Tumor Growth**

Given that knocking down lncRNA SSTR5-AS1 can play an anti-OC role in cell experiments, this study will be verified by transplanted tumor nude mice. SKOV3 cells stably transfected with sh-SSTR5-AS1 and OE-SSTR5-AS1 were subcutaneously injected into the dorsal side of mice. *lncRNA SSTR5-AS1* level was significantly decreased when sh-SSTR5-AS1 intervention and significantly raised when OE-SSTR5-AS1 intervention (Figure 7A), indicating that *lncRNA SSTR5-AS1* level in mice was successfully interfered. The tumor volumes were tested weekly throughout the experiment; the tumors were stripped after 5 weeks. The weight and volume of transplanted tumor were markedly lessened when downregulation of lncRNA SSTR5-AS1 knockdown, and significantly increased after lncRNA SSTR5-AS1 overexpression (Figure 7B–D). Immunohistochemical results found that knocking down lncRNA SSTR5-AS1 obviously reduced Ki-67 positive cells (Figure 7E–F); DCFH-DA fluorescent probe results found that knocking down lncRNA SSTR5-AS1 obviously increased ROS levels (Figure

7G). Overexpression of lncRNA SSTR5-AS1 had the opposite effect. The Perls reaction is a classic histochemical method. To demonstrate a sensitive and traditionally excellent detection method for Fe<sup>3+</sup> in tissues, this method relies on the reaction of Fe<sup>3+</sup> with potassium ferrocyanide, which forms an insoluble blue compound. There are many blue iron particles deposited in the sh-SSTR5-AS1 group, showing obvious iron deposition. The OE-SSTR5-AS1 group has a small amount of iron deposition, only a few blue iron particles are deposited (Figure 7H). After downregulation of lncRNA SSTR5-AS1 knockdown, the contents of IL-10 (reduced by 75%), TGF-β (reduced by 70%), IL-4 (reduced by 50%), and IL-35 (reduced by 53%) were significantly decreased (Figure 7I–L), and p-STAT3/STAT3 (reduced by 74%), SLC7A11 (reduced by 54%), FTH1 (reduced by 52%), Nrf2 (reduced by 49%), and GPX4 (reduced by 49%) proteins were also significantly decreased (Figure 7M–R); the levels of the above indicators were significantly increased after lncRNA SSTR5-AS1 overexpression (Figure 7I–R). In summary, downregulation of lncRNA SSTR5-AS1 inhibited the STAT3/SLC7A11 signaling pathway, induced ferroptosis, reduced the secretion of immunosuppressive factors, and inhibited the growth of OC tumors.



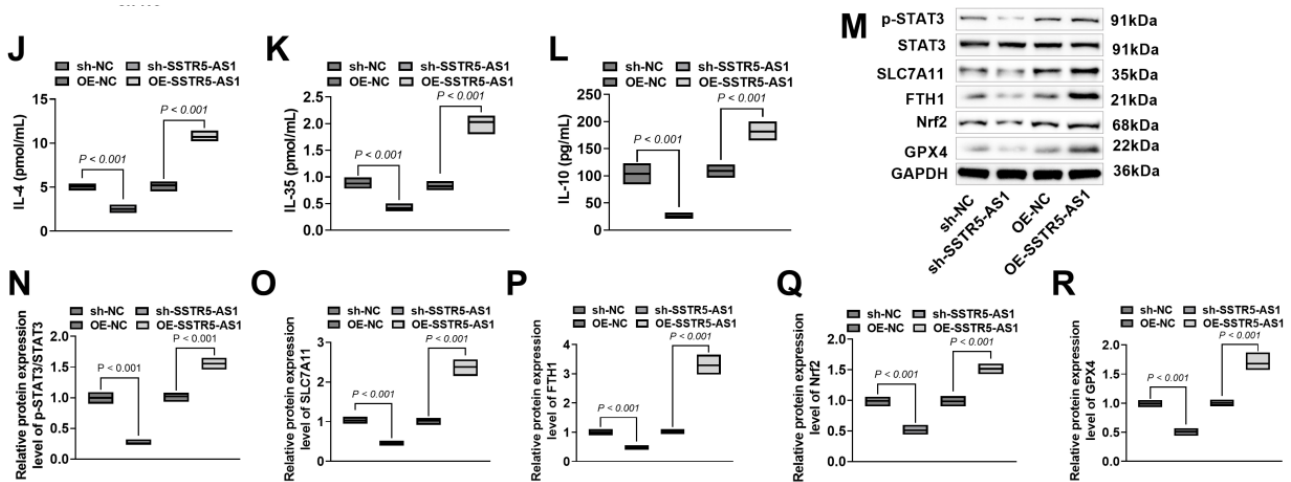


**Figure 7.** In vivo experiments. A, SKOV3 cells stably transfected with sh-SSTR5-AS1, sh-NC, OE-SSTR5-AS1, and OE-NC ( $2 \times 10^5$  cells) were subcutaneously injected into the dorsal side of nude mice. *lncRNA SSTR5-AS1* expression in tumor tissues was measured using RT-qPCR. B–D, Weekly tumor volume and tumor weight on day 35. sh-SSTR5-AS1 significantly lessened tumor weight and volume. E, The representative figure of Ki-67 immunohistochemistry, DCFH-DA staining, and Prussian blue staining ( $\times 40$ ,  $50 \mu\text{m}$ ). F, Ki-67 expression was detected by immunohistochemistry, which was significantly reduced after downregulation of *lncRNA SSTR5-AS1* knockdown. G, DCFH-DA fluorescent probe detected ROS levels of tumor tissues. sh-SSTR5-AS1 significantly increased ROS levels. H, Prussian blue staining examined iron deposition in tissue sections. sh-SSTR5-AS1 group had obvious iron deposition. I–L, The content of immunosuppressive factors was examined by ELISA kit. IL-10, TGF- $\beta$ , IL-4, and IL-35 contents decreased after downregulation of *lncRNA SSTR5-AS1* knockdown. M–R, Western blot detected ferroptosis and STAT3/SLC7A11 pathway protein levels in tumor tissues. p-STAT3/STAT3, SLC7A11, FTH1, Nrf2, and GPX4 proteins decreased after downregulation of *lncRNA SSTR5-AS1* knockdown.  $n=6$ ,  $***p<0.001$  vs sh-NC group;  $###p<0.001$  vs OE-NC group.

## DISCUSSION

The functions and mechanism of *lncRNA* for OC progression may provide assistance in developing new therapeutic strategies for OC. Recently, *lncRNA SSTR5-AS1* exerts anti-tumor effects through impacting the growth, EMT, apoptosis, and metastasis of cancer cells. Yuan et al<sup>24</sup> showed that *lncRNA SSTR5-AS1* was overexpressed at prostate cancer, the high *lncRNA* level was related to tumor stage and lymph node metastasis. The increase in the level of this indicator may be an independently poor prognostic factor for patients with prostate cancer.<sup>24</sup> In esophageal cancer, *lncRNA SSTR5-AS1* regulates the ITGB6/JAK1/STAT3 signaling axis by interacting with eukaryotic translation initiation factor 4A3 (EIF4A3) to promote tumor development.<sup>23</sup> Cheng et al<sup>25</sup> pointed out that *lncRNA SSTR5-AS1* was raised at gastric cancer, and high expression of this *lncRNA* was associated with distant metastasis and TNM stage.<sup>25</sup> This indicates that *lncRNA SSTR5-AS1* may play a role in promoting cancer.

Consistent with previous studies, in this study, *lncRNA SSTR5-AS1* was raised on OC, and was present in the cytoplasm of OC. *lncRNA SSTR5-AS1* overexpressed increased the cell viability, migration and invasion cell number and cell migration rate, and the increased expression of key regulatory genes MMP-2 and MMP-9 also further confirmed the positive regulation of *lncRNA* on OC movement and invasion. Knockdown of *lncRNA SSTR5-AS1* suppressed OC cell growth, movement, and invasion. *lncRNA SSTR5-AS1* is associated with OC development, and knockdown of *lncRNA SSTR5-AS1* may play a cancer-suppressive role.

Tumor microenvironment is mainly controlled by immunosuppressive cytokines. Among many immunosuppressive cytokines, IL-10, TGF- $\beta$ , IL-4, and IL-35 are dominant in the tumor environment of various tumors and are primarily involved in immunosuppression.<sup>29</sup> Recent studies have shown that these cytokines are important for restricting anti-tumor immunity and tumor growth progressions; blocking immunosuppressive cytokines may play a remarkable

## Knockdown of LncRN SSTR5-AS1 Interferes with Ovarian Cancer Progression

effect in sensitizing tumors to immunotherapy, thereby regulating tumorigenesis.<sup>29,30</sup> In this study, we observed that knockdown of lncRNA SSTR5-AS1 significantly down-regulated IL-10, TGF- $\beta$ , IL-4, and IL-35 expressions, indicating that knocking down lncRNA SSTR5-AS1 reduced immunosuppressive cytokines in the tumor microenvironment. Studies have confirmed that one of the mechanisms that cause OC's therapeutic resistance and immunosuppression is to increase the expression of immunosuppressive cytokine IL-10.<sup>31</sup> Therefore, knockdown of lncRNA SSTR5-AS1 can slow down the malignant progression of OC by inhibiting immunosuppressive cytokines and improving the immune response of tumor cells.

Ferroptosis is essential for inhibiting tumor progression. Fe<sup>2+</sup> is one of the key factors that directly promote cell death in lipid peroxidation, and is also a typical marker of ferroptosis.<sup>32</sup> The accumulation of Fe<sup>2+</sup> can trigger lipid peroxidation of cell membrane, induce high levels of oxidative stress in cells, lead to a large accumulation of ROS and MDA, inhibit the level of GSH, and ultimately lead to cell death.<sup>33</sup> Zhang et al<sup>34</sup> showed that squalene monooxygenase can reduce ROS and lipid peroxides, protect OC cells from ferroptosis.<sup>34</sup> Zhao et al<sup>35</sup> found that Obacunone could increase cellular iron content and MDA level, and induce ferroptosis in OC cells.<sup>35</sup> Knockdown of lncRNA SSTR5-AS1 could significantly increase intracellular Fe<sup>2+</sup>, MDA, and ROS levels and inhibit GSH levels, suggesting that knockdown of lncRNA SSTR5-AS1 could promote lipid peroxidation of SKOV3 and A2780 cells and induce ferroptosis. Next, this research examined changes in key indicators of ferroptosis process. Nrf2 level is related to ferroptosis. Increasing of Nrf2 protein significantly inhibits ferroptosis occurrence, and downregulation of Nrf2 expression will promote ferroptosis.<sup>36</sup> The expression of FTH1 is closely related to iron metabolism during ferroptosis. GPX4 can inhibit intracellular lipid peroxidation and prevent ferroptosis.<sup>37</sup> Knockout of GPX4 in wild-type mice directly triggered ferroptosis initiation.<sup>38</sup> Downregulation of SLC7A11 expression can promote the accumulation of lipid peroxides, resulting in a decrease in GSH production and inhibition of GPX4, thereby inducing ferroptosis.<sup>39</sup> Nrf2, SLC7A11, FTH1, and GPX4 protein expressions were significantly lessened when knockdown of lncRNA SSTR5-AS1, which further proved that knockdown of lncRNA SSTR5-AS1 induced ferroptosis in OC cells. Ferroptosis

is an important way of cell death. The US FDA has now approved ferroptosis inducers represented by sorafenib for the treatment of malignant tumors, which fully demonstrates the great potential of ferroptosis in the development of new anti-tumor drugs,<sup>40</sup> and also highlights the development value of lncRNA based on ferroptosis in this study. Recent studies have found that ferroptosis-related lncRNA can be used as a prognostic biomarker for OC.<sup>41,42</sup> In gynecological malignancies, a recent meta-analysis evaluated the prognostic value of core ferroptosis regulators.<sup>43,44</sup> The high expression of SLC7A11 and GPX4 is associated with poor overall survival in cancer patients,<sup>45,46</sup> highlighting their role in disease progression and treatment resistance. Future studies that correlate lncRNA SSTR5-AS1 levels with the characteristics of ferroptosis biomarkers established in the patient cohort can further verify its potential as a complementary predictor.

STAT3 promises a possible therapeutic target for OC.<sup>47</sup> Inhibiting STAT3 pathway can increase ROS levels and inhibit OC growth and metastasis.<sup>48,49</sup> Moreover, STAT3 has been shown to be a key factor in regulating lipid peroxidation in tumor cells.<sup>50</sup> It has been reported that there is a binding site between STAT3 and the promoter region of SLC7A11.<sup>51</sup> Inhibition of STAT3 can reduce ferroptosis important factors GPX4 and SLC7A11 levels, and then mediate the metabolic abnormalities of amino acids such as cysteine to trigger GSH synthesis depletion, and ultimately induce ferroptosis.<sup>32</sup> Mo et al<sup>52</sup> pointed out that iron overload can inhibit the STAT3/SLC7A11 signaling pathway and induce liver ferroptosis.<sup>52</sup> Yang et al<sup>53</sup> showed that AKR1B1 interacts with STAT3 to activate SLC7A11, inhibits ferroptosis and promotes gastric cancer progression.<sup>53</sup> Inhibition of the STAT3/SLC7A11 pathway can induce ferroptosis, thereby reducing the growth of hepatocellular carcinoma and osteosarcoma.<sup>28,54</sup> Similar to previous researches, the results of this study found that after lncRNA SSTR5-AS1 knockdown was accompanied by significant reductions in the protein levels of p-STAT3/STAT3 and SLC7A11, suggesting a potential association between lncRNA SSTR5-AS1 and the STAT3/SLC7A11 axis. And RIP experiments demonstrated the interaction between lncRNA SSTR5-AS1 and STAT3. To distinguish correlation from causation and verify that lncRNA SSTR5-AS1 affects OC cells primarily through this pathway, we conducted functional rescue experiments. By overexpressing STAT3 in lncRNA

SSTR5-AS1-knockdown cells, we found that overexpression of STAT3 partially reversed the induction of ferroptosis and the inhibitory effects on cell growth, migration, invasion and immunosuppressive factor expression via knockdown of lncRNA SSTR5-AS1 in OC cells, knocking down STAT3 had the opposite effect. These experiments demonstrate that the activation of the STAT3/SLC7A11 pathway is a key downstream causal mechanism by which lncRNA SSTR5-AS1 regulates ferroptosis and malignant behaviors in OC cells.

Finally, SKOV3 cells stably transfected with sh-SSTR5-AS1 and OE-SSTR5-AS1 were subcutaneously injected into the back of mice to establish a transplanted tumor model. Knocking down lncRNA SSTR5-AS1 notably reduced tumor weight, inhibited the growth of OC *in vivo*, and reduced the content of immunosuppressive factors. After lncRNA SSTR5-AS1 was knocked down, there was obvious iron deposition in tumor tissue, ROS level increased significantly, ferroptosis protein decreased significantly, and STAT3/SLC7A11 signaling pathway was inhibited. In summary, downregulation of lncRNA SSTR5-AS1 inhibited STAT3/SLC7A11 signaling pathway, induced ferroptosis, reduced the secretion of immunosuppressive factors, and suppressed the growth of OC tumors.

This study found that lncRNA SSTR5-AS1 inhibits ferroptosis by activating the STAT3/SLC7A11 axis, thereby driving the progression of OC, which provides an important clue for its clinical transformation. Unfortunately, this study mainly relies on two OC cells, SKOV3 and A2780. In the future, it needs to be verified in a more diversified OC cell model, especially the more representative high-grade serous OC (HGSOC) cell line and cisplatin and other chemotherapeutic drug-resistant cell lines. Secondly, there is inherent molecular heterogeneity between different cell lines, which may affect the regulatory strength and downstream effects of the lncRNA SSTR5-AS1/STAT3/SLC7A11 pathway. Therefore, the acceptance of this conclusion needs to be further confirmed and expanded in the future through a wider range of cell models and clinical sample analysis. Although this study did not directly carry out clinical cohort analysis, the above mechanism suggests that the high expression of lncRNA SSTR5-AS1 may indicate abnormal activation of STAT3 pathway and ferroptosis resistance, which is related to the poor prognosis and potential therapeutic resistance of patients. Future studies can verify the association between lncRNA

SSTR5-AS1 expression and the survival of OC patients by analyzing public databases such as TCGA; at the same time, given that tumors with high expression of lncRNA SSTR5-AS1 show decreased ferroptosis sensitivity, its expression level may be used as a potential biomarker to predict the response of tumors to emerging ferroptosis inducers. Future work will be verified by analyzing clinical cohort data to provide a basis for the development of precise treatment strategies for this molecular subtype.

Overall, knockdown of lncRNA SSTR5-AS1 can significantly suppress the multiplication, migration, invasion, and immunosuppressive factors of OC. Its mechanism is associated with STAT3/SLC7A11 pathway regulation and ferroptosis induction. This study reveals the anti-OC effect and molecular mechanism of knockdown of lncRNA SSTR5-AS1, and provides experimental support for the design of clinical trials and clinical application transformation. However, considering the complex causes of OC formation and individual differences, this study still needs to be further explained and verified based on a variety of different species and types of OC *in vitro* and *in vivo* models.

#### STATEMENT OF ETHICS

This study was approved by Wuhan Third Hospital (Tongren Hospital of Wuhan University) Ethic Committee (Approval number: 2024-018).

#### FUNDING

Wuhan Medical Science Research Project. (No. WX23Z17).

#### CONFLICT OF INTEREST

The authors declare no conflicts of interest.

#### ACKNOWLEDGMENTS

Not applicable

#### DATA AVAILABILITY

The data supporting the findings of this study can be obtained from the corresponding author, upon request.

## AI ASSISTANCE DISCLOSURE

Not applicable.

## REFERENCES

1. Pal S, Bhowmick S, Sharma A, Sierra-Fonseca JA, Mondal S, Afolabi F, et al. Lymphatic vasculature in ovarian cancer. *Biochim Biophys Acta Rev Cancer*. 2023;1878(5):188950.
2. Wang X, Zhou Y, Zhou X, Zhang B, Liang H, Chen Y. tsRNA-Ala-3-0030 drives ovarian cancer progression by suppressing ZNF70. *Front Oncol*. 2026;29:1738006.
3. Han B, Zheng R, Zeng H, Wang S, Sun K, Chen R, et al. Cancer incidence and mortality in China, 2022. *J National Cancer Center*. 2024;4(1):47-53.
4. Chan JK, Tian C, Kesterson JP, Monk BJ, Kapp DS, Davidson B, et al. Symptoms of Women With High-Risk Early-Stage Ovarian Cancer. *Obstet Gynecol*. 2022;139(2):157-62.
5. Akter S, Rahman MA, Hasan MN, Akhter H, Noor P, Islam R, et al. Recent Advances in Ovarian Cancer: Therapeutic Strategies, Potential Biomarkers, and Technological Improvements. *Cells*. 2022;11(4): 650.
6. Ogasawara A, Sato S, Hasegawa K. Current and future strategies for treatment of ovarian clear cell carcinoma. *J Obstet Gynaecol Res*. 2020;46(9):1678-89.
7. Konstantinopoulos PA, Matulonis UA. Clinical and translational advances in ovarian cancer therapy. *Nat Cancer*. 2023;4(9):1239-57.
8. Yapici FI, Bebbler CM, von Karstedt S. A guide to ferroptosis in cancer. *Mol Oncol*. 2024;18(6):1378-96.
9. Singh M, Arora HL, Naik R, Joshi S, Sonawane K, Sharma NK, et al. Ferroptosis in Cancer: Mechanism and Therapeutic Potential. *Int J Mol Sci*. 2025;26(8):3852.
10. Su C, Xue Y, Fan S, Sun X, Si Q, Gu Z, et al. Ferroptosis and its relationship with cancer. *Front Cell Developmental Biol*. 2024;12:1423869.
11. Wang CK, Chen TJ, Tan GYT, Chang FP, Sridharan S, Yu CA, et al. MEX3A Mediates p53 Degradation to Suppress Ferroptosis and Facilitate Ovarian Cancer Tumorigenesis. *Cancer Res*. 2023;83(2):251-63.
12. Chen B, Zhao L, Yang R, Xu T. The recent advancements of ferroptosis in the diagnosis, treatment and prognosis of ovarian cancer. *Front Genet*. 2023;9(14):1275154.
13. Cang W, Wu A, Gu L, Wang W, Tian Q, Zheng Z, et al. Erastin enhances metastatic potential of ferroptosis-resistant ovarian cancer cells by M2 polarization through STAT3/IL-8 axis. *Int Immunopharmacol*. 2022;113(Pt B):109422.
14. Zhao L, Zhou X, Xie F, Zhang L, Yan H, Huang J, et al. Ferroptosis in cancer and cancer immunotherapy. *Cancer Commun*. 2022;42(2):88-116.
15. Zhao H, Xu Y, Shang H. Ferroptosis: A New Promising Target for Ovarian Cancer Therapy. *Int J Med Sci*. 2022;19(13):1847-55.
16. Yuan Y, Tang Y, Fang Z, Wen J, Wicha MS, Luo M. Long Non-Coding RNAs: Key Regulators of Tumor Epithelial/Mesenchymal Plasticity and Cancer Stemness. *Cells*. 2025;14(3):227.
17. Li J, Wang X, Wang H. RNA modifications in long non-coding RNAs and their implications in cancer biology. *Bioorg Med Chem*. 2024;113(8):117922.
18. Coan M, Haefliger S, Ounzain S, Johnson R. Targeting and engineering long non-coding RNAs for cancer therapy. *Nat Rev Gen*. 2024;25(8):578-95.
19. Lin H, Xu X, Chen K, Fu Z, Wang S, Chen Y, et al. LncRNA CASC15, MiR-23b Cluster and SMAD3 form a Novel Positive Feedback Loop to promote Epithelial-Mesenchymal Transition and Metastasis in Ovarian Cancer. *Int J Biol Sci*. 2022;18(5):1989-2002.
20. Basu S, Nadhan R, Dhanasekaran DN. Long Non-Coding RNAs in Ovarian Cancer: Mechanistic Insights and Clinical Applications. *Cancers*. 2025;17(3):472.
21. Xue Z, Yang B, Xu Q, Zhu X, Qin G. Long non-coding RNA SSTR5-AS1 facilitates gemcitabine resistance via stabilizing NONO in gallbladder carcinoma. *Biochem Biophys Res Commun*. 2020;522(4):952-9.
22. Hu Y, Mao N, Zheng W, Hong B, Deng X. LncRNA SSTR5-AS1 Predicts Poor Prognosis and Contributes to the Progression of Esophageal Cancer. *Dis Markers*. 2023;2023:5025868.
23. Tang Z, Jiang Y, Zong Y, Ding S, Wu C, Tang Z, et al. LncRNA SSTR5-AS1 promotes esophageal carcinoma through regulating ITGB6/JAK1/STAT3 signaling. *Epigenomics*. 2024;16(17):1133-48.
24. Yuan S, Bi J, Zhang Y. LncRNA SSTR5-AS1 as a Prognostic Marker Promotes Cell Proliferation and Epithelial-to-Mesenchymal Transition in Prostate Cancer. *Crit Rev Eukaryot Gene Expr*. 2023;33(2):1-12.
25. Cheng Y, Di J, Wu J, Shi HT, Zou BC, Zhang Y, et al. Diagnostic and prognostic significance of long noncoding RNA SSTR5-AS1 in patients with gastric cancer. *Eur Rev Med Pharmacol Sci*. 2020;24(10):5385-90.
26. Yang XC, Jin YJ, Ning R, Mao QY, Zhang PY, Zhou L, et al. Electroacupuncture attenuates ferroptosis by promoting Nrf2 nuclear translocation and activating

- Nrf2/SLC7A11/GPX4 pathway in ischemic stroke. *Chinese Med.* 2025;20(1):4.
27. Wang M, Zheng HS, Ye WL, Mao JD, Zhang K, Yang L, et al. The mechanism of electroacupuncture-mediated improvement in Parkinson's disease by inhibiting ferroptosis through activating the Nrf2/GPX4 signal pathway. *Front Aging Neurosci.* 2025;17:1551404.
  28. Chen L, Sun R, Fang K. Erianin inhibits tumor growth by promoting ferroptosis and inhibiting invasion in hepatocellular carcinoma through the JAK2/STAT3/SLC7A11 pathway. *Pathol Int.* 2024;74(3):119-28.
  29. Mirlekar B. Tumor promoting roles of IL-10, TGF- $\beta$ , IL-4, and IL-35: Its implications in cancer immunotherapy. *SAGE Open Med.* 2022;10:20503121211069012.
  30. Liu K, Huang A, Nie J, Tan J, Xing S, Qu Y, et al. IL-35 Regulates the Function of Immune Cells in Tumor Microenvironment. *Front Immunol.* 2021;12:683332.
  31. Martincuks A, Song J, Kohut A, Zhang C, Li YJ, Zhao Q, et al. PARP Inhibition Activates STAT3 in Both Tumor and Immune Cells Underlying Therapy Resistance and Immunosuppression In Ovarian Cancer. *Front Oncol.* 2021;11:724104.
  32. Ouyang S, Li H, Lou L, Huang Q, Zhang Z, Mo J, et al. Inhibition of STAT3-ferroptosis negative regulatory axis suppresses tumor growth and alleviates chemoresistance in gastric cancer. *Redox Biol.* 2022;52:102317.
  33. Yang R, Gao W, Wang Z, Jian H, Peng L, Yu X, et al. Polyphyllin I induced ferroptosis to suppress the progression of hepatocellular carcinoma through activation of the mitochondrial dysfunction via Nrf2/HO-1/GPX4 axis. *Phytomedicine.* 2024;122:155135.
  34. Zhang R, Zhang L, Fan S, Wang L, Wang B, Wang L. Squalene monooxygenase (SQLE) protects ovarian cancer cells from ferroptosis. *Sci Reports.* 2024;14(1):22646.
  35. Zhao Y, Liang H, Cui X. Obacunone regulates ferroptosis in ovarian cancer through the Akt/p53 pathway. *Naunyn Schmiedebergs Arch Pharmacol.* 2025;398(6):7027-39.
  36. Liu D, Zhu Y. Unveiling Smyd-2's Role in Cytoplasmic Nrf-2 Sequestration and Ferroptosis Induction in Hippocampal Neurons After Cerebral Ischemia/Reperfusion. *Cells.* 2024;13(23):1969.
  37. Yao D, Bao L, Wang S, Tan M, Xu Y, Wu T, et al. Isoliquiritigenin alleviates myocardial ischemia-reperfusion injury by regulating the Nrf2/HO-1/SLC7a11/GPX4 axis in mice. *Free Radic Biol Med.* 2024;221:1-12.
  38. Xu Y, Chen J, Zhou L, Zhao Y, He N, Xu Q, et al. Gastrodin Protects Against Sepsis-Associated Encephalopathy By Suppressing Ferroptosis. *Shock (Augusta, Ga).* 2025;63(4):628-37.
  39. Ursini F, Maiorino M. Lipid peroxidation and ferroptosis: The role of GSH and GPx4. *Free Radic Biol Med.* 2020;152:175-85.
  40. Zhou TJ, Zhang MM, Liu DM, Huang LL, Yu HQ, Wang Y, et al. Glutathione depletion and dihydroorotate dehydrogenase inhibition actuated ferroptosis-augment to surmount triple-negative breast cancer. *Biomaterials.* 2024;305:122447.
  41. Wang K, Mei S, Cai M, Zhai D, Zhang D, Yu J, et al. Ferroptosis-Related Long Noncoding RNAs as Prognostic Biomarkers for Ovarian Cancer. *Front Oncol.* 2022;12:888699.
  42. Zheng J, Guo J, Wang Y, Zheng Y, Zhang K, Tong J. Bioinformatic Analyses of the Ferroptosis-Related lncRNAs Signature for Ovarian Cancer. *Front Mol Biosciences.* 2021;8:735871.
  43. Li S, Tao K, Yun H, Yang J, Meng Y, Zhang F, et al. Ferroptosis is a protective factor for the prognosis of cancer patients: a systematic review and meta-analysis. *BMC Cancer.* 2024;24(1):604.
  44. Han S, Wang S, Lv X, Li D, Feng Y. Ferroptosis-related genes in cervical cancer as biomarkers for predicting the prognosis of gynecological tumors. *Front Mol Biosciences.* 2023;10:1188027.
  45. Fantone S, Piani F, Olivieri F, Rippo MR, Sirico A, Di Simone N, et al. Role of SLC7A11/xCT in Ovarian Cancer. *Int J Mol Sci.* 2024;25(1):587.
  46. Wu H, Liao X, Huang W, Hu H, Lan L, Yang Q, et al. Examining the prognostic and clinicopathological significance of GPX4 in human cancers: a meta-analysis. *Free Radic Res.* 2025;59(3):239-49.
  47. Liang R, Chen X, Chen L, Wan F, Chen K, Sun Y, et al. STAT3 signaling in ovarian cancer: a potential therapeutic target. *J Cancer.* 2020;11(4):837-48.
  48. Li Q, Yang F, Shi X, Bian S, Shen F, Wu Y, et al. MTHFD2 promotes ovarian cancer growth and metastasis via activation of the STAT3 signaling pathway. *FEBS Open Bio.* 2021;11(10):2845-57.
  49. Wu K, Qiu C, Ma Q, Chen F, Lu T. The anti-cancer mechanism of Celastrol by targeting JAK2/STAT3 signaling pathway in gastric and ovarian cancer. *Toxicol Applied Pharmacol.* 2024;491:117077.
  50. Wu K, Liu L, Wu Z, Huang Q, Zhou L, Xie R, et al. Ascorbic acid induces ferroptosis via STAT3/GPX4

## Knockdown of LncRN SSTR5-AS1 Interferes with Ovarian Cancer Progression

signaling in oropharyngeal cancer. *Free Radic Res.* 2024;58(2):117-29.

Axis in Osteosarcoma Cells. *Oxid Med Cell Longev.* 2021;2021:1783485.

51. Huang CY, Chen LJ, Chen G, Chao TI, Wang CY. SHP-1/STAT3-Signaling-Axis-Regulated Coupling between BECN1 and SLC7A11 Contributes to Sorafenib-Induced Ferroptosis in Hepatocellular Carcinoma. *Int J Mol Sci.* 2022;23(19):11092.
52. Mo M, Pan L, Deng L, Liang M, Xia N, Liang Y. Iron Overload Induces Hepatic Ferroptosis and Insulin Resistance by Inhibiting the Jak2/stat3/slc7a11 Signaling Pathway. *Cell Biochemistry Biophysics.* 2024;82(3):2079-94.
53. Yang K, Zhang X, Long F, Dai J. AKR1B1 Inhibits Ferroptosis and Promotes Gastric Cancer Progression via Interacting With STAT3 to Activate SLC7A11. *Cell Biol Int.* 2025;49(4):374-83.
54. Luo Y, Gao X, Zou L, Lei M, Feng J, Hu Z. Bavachin Induces Ferroptosis through the STAT3/P53/SLC7A11

IMPRESSIONS